

A method of phase demodulation of OFDR based on ARC-DSM algorithm*

LIU Jianfei^{1**}, LI Chao¹, FAN Xujun¹, LUO Mingming¹, LUAN Nannan¹, and YANG Wenrong²

1. School of Electronic Information Engineering, Hebei University of Technology, Tianjin 300401, China

2. State Key Laboratory of Reliability and Intelligence of Electrical Equipment, Hebei University of Technology, Tianjin 300130, China

(Received 21 May 2021; Revised 15 July 2021)

©Tianjin University of Technology 2022

Aiming at low stability and high harmonic distortion of the traditional phase-generated carrier (PGC) demodulation algorithm, we propose a modified demodulation algorithm for distributed strain sensing in phase-sensitive optical frequency domain reflectometry (OFDR). The proposed algorithm combines the arctangent function and differential-self-multiplying (ARC-DSM), which eliminates the effect of modulation depth and realizes the high precision strain variation measurements. Simulation results show that distortion and harmonic distortion are effectively suppressed by the ARC-DSM algorithm. The minimum variation of the measurable static strain is about $0.3\mu\epsilon$ and the spatial resolution can reach 0.2 m within 270 m range.

Document code: A **Article ID:** 1673-1905(2022)01-0013-5

DOI <https://doi.org/10.1007/s11801-022-1083-0>

Distributed fiber strain sensing has the advantages of distributed measurement capability, high spatial resolution, high precision, and light in weight, are widely used in health monitoring, 3D shape sensing, refractive index, airplane wings, etc^[1]. As one of the optical fiber sensing technologies, due to its high spatial resolution, high sensitivity, and high signal to noise ratio, optical frequency domain reflectometry (OFDR) has attracted more and more attention since EICKHOFF^[2] firstly proposed it in 1981. In OFDR, the demodulation algorithm is critical to improve the measurement accuracy of sensing system^[3].

FROGGATT and MOORE^[4] applied OFDR to distributed static strain measurement, with fast Fourier transformation (FFT) based demodulation in frequency domain, which can qualitatively locate and observe strain. Then researchers proposed various demodulation methods to improve the performance of strain detection. The method of measuring Rayleigh backscattering spectrum (RBS) shift by cross-correlation calculation is adopted in OFDR. Based on this demodulation method, CHEN et al^[5] used a time-gated digital (TGD) OFDR system to perform strain detection, which realizes a minimum measured strain of $1\mu\epsilon$. However, cross-correlation calculation demodulation is susceptible to the influence of the reference signal, so it is easy to cause a measurement error. Another approach is based on the phase shift induced by the strain variation^[6]. Phase-sensitive OFDR can directly demodulate strain information by analyzing

the phase change of Rayleigh backscattering light. Phase-generated carrier (PGC) is a typical phase demodulation algorithm^[7]. PGC has many advantages, such as high detection sensitivity, large dynamic range, and high phase measurement accuracy^[8]. The U.S. Naval Laboratory first applied the PGC demodulation algorithm to optical fiber sensors^[9]. The traditional PGC demodulation algorithms employ the phase-generated carrier differential-and-cross-multiplying (PGC-DCM)^[10] and the phase generated carrier arctangent function (PGC-ARC)^[11]. However, the PGC-DCM demodulation algorithm is influenced by the light intensity and phase modulation depth^[12]. Although the PGC-ARC algorithm proposed later can eliminate the effect of light intensity, modulation depth still leads to nonlinear or serious harmonic distortion of the demodulation results.

In this paper, we present a distributed high precision strain sensing method based on phase-sensitive OFDR. By analyzing the phase variation of Rayleigh backscattered light, a new ARC-DSM algorithm based phase demodulation is proposed to obtain accurate phase information, which can eliminate the influence of modulation depth on demodulation results and obtain demodulation results satisfying the requirements. This method has both high stability and low harmonic distortion, which can realize high precision strain sensing directly.

When a linear frequency scanning coherent light provided by the tunable laser source (TLS) is injected into

* This work has been supported by the National Natural Science Foundation of China (No.51077037), the Natural Science Foundation of Hebei Province (Nos.F2019202294 and A2020202013), and the Natural Science Foundation of Tianjin City (No.15JCYBJC17000).

** E-mail: jfliu@hebut.edu.cn

the sensing fiber, the beat signal of OFDR is formed by the beat interference of two reflected optical signals. Among them, the light field of the reference signal can be expressed as

$$E_r(t) = E_0 \exp \{ j[2\pi f_0 t + \pi k_r t^2 + e(t)] \}, \quad (1)$$

where E_0 is the intensity of the light field, f_0 is the initial frequency, k_r is the tuning rate of the tunable laser source, and $e(t)$ is the phase noise or nonlinear phase. The optical field of the signal to be measured is denoted as

$$E_s(t) = \sqrt{R(\tau)} E_0 \exp \{ j[2\pi f_0(t - \tau) + \pi k_r(t - \tau)^2 + e(t - \tau)] \}, \quad (2)$$

where τ is the signal delay of the circuit to be tested. The beating signal^[11] is

$$E(t) = 2\sqrt{R(\tau)} E_0 \exp \{ j2\pi[f_0\tau + k_r\tau t - \frac{1}{2}k_r\tau^2 + e(t) - e(t - \tau)] \}, \quad (3)$$

where $e(t) - e(t - \tau)$ is the phase noise of beat frequency signal. It's worth noting that as long as the measurement range is within the laser coherence length, the third term of Eq.(3) can be ignored.

The PGC modulation and demodulation technology is a homodyne method with broad application prospects. It has high sensitivity, large dynamic range, strong anti-noise ability and can avoid the random phase fading. According to the structure, the traditional PGC demodulation algorithm can be divided into the DCM algorithm and the ARC algorithm.

The result of DCM is obtained as^[10]

$$I(t) = DB^2 GHJ_1(C)J_2(C)\cos(w_s t), \quad (4)$$

where D is a constant, B is related to the polarization state change, C is the PGC phase modulation depth, w_s is the PGC modulation angular frequency, G is the amplitude of the fundamental frequency signal of the carrier signal, H is the double frequency signal amplitude of the carrier signal, and $J_1(C)J_2(C)$ is mainly affected by the modulation depth parameter, which has low stability when the light intensity changes rapidly.

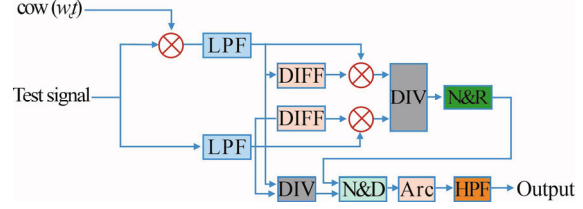
For ARC demodulation algorithm, the first part is the same as the DCM method. Then it divides the two signals after the band-pass filter, so the result of ARC algorithm is obtained as^[11]

$$I(t) = \arctan \left[\frac{GJ_1(C)}{HJ_2(C)} \tan \varphi(t) \right]. \quad (5)$$

Based on the analysis above, we can find that $J_1(C)$ and $J_2(C)$ are no longer equal when C deviates from 2.63, thus leads a high harmonic distortion, and the amplitude of the demodulated signal is still affected by the modulation parameter C .

In this paper, the OFDR strain demodulation algorithm is proposed based on the combination of differential-self-multiplication and arctangent algorithm. Although the computational complexity of the system is increased, the algorithm can achieve signal demodulation effec-

tively and avoid the influence of modulation depth. The principle of basic frequency ARC-DSM algorithm is shown in Fig.1.



LPF: low-pass-filter; DIFF: differentiator; DIV: divider; N&R: negative and root; N&D: negative and divider; HPF: high-pass-filter

Fig.1 Principle of basic frequency ARC-DSM algorithm

When there is the strain in the optical fiber, the relation between phase change $\Delta\phi(t)$ and strain $\varepsilon(t)$ can be expressed as^[12]

$$n_g k_0 \zeta_v L \varepsilon(t) = \Delta\phi(t) + 2n\pi, \quad (6)$$

where n_g is the fiber group index, k_0 is the number of light waves and ζ_v is the strain coefficient of composite fiber. Since phase change is a periodic process, the larger strain may lead to an excess phase change^[13]. At this point, the OFDR signal can be expressed as

$$E(t) = 2\sqrt{R(\tau)} E_0^2 \cos \left[2\pi \left(f_0\tau + k_r\tau t - \frac{1}{2}k_r\tau^2 \right) + \Delta\phi(t) \right]. \quad (7)$$

OFDR signals are divided into two channels, one of which is multiplied by the fundamental frequency signal and passes through the lowpass filter, and the other is directly passed through the lowpass filter. The modulated signals are represented by Bessel function. Two signals can be expressed as

$$I_1(t) = -BJ_1(C)\sin[\Delta\phi(t)], \quad (8)$$

$$I_2(t) = BJ_2(C)\cos[\Delta\phi(t)], \quad (9)$$

where $J_1(C)$ and $J_2(C)$ are the first-order and second-order Bessel functions about the modulation depth C . Then, the differential and self-multiplication are performed on the signals of the two channels. Finally, the signals of the two channels are divided and taken the negative joint square root. The coefficients of Bessel function are obtained as follows

$$\kappa = \frac{J_1(C)}{J_2(C)}. \quad (10)$$

In addition, the two-channel signal division after low-pass filtering can be obtained as follows

$$\phi(t) = -\frac{J_1(C)}{J_2(C)} \tan[\Delta\phi(t)], \quad (11)$$

where $\Delta\phi(t)$ is the phase to be measured. Dividing Eq.(11) by Eq.(10) and taking the negative into the arctangent function, we can get

$$\Delta\phi(t) = \arctan \left[-\frac{\varphi(t)}{\kappa} \right]. \quad (12)$$

Thus, the phase information can be demodulated. Finally, the strain can be obtained as follows

$$\varepsilon(t) = \frac{\Delta\phi(t) + 2n\pi}{n_g k_0 \xi_v L}. \quad (13)$$

A phase-sensitive OFDR simulation system was established on MATLAB platform. Aiming at the tuning nonlinearity of laser source in OFDR system, a nonlinear compensation algorithm based on polynomial regression algorithm (PRA)^[14] is adopted. We mainly introduce the setting and results of the simulation, as well as the detailed analysis of simulation results.

Fig.2 illustrates the simulation structure of OFDR system mainly consisting of the main interferometer and auxiliary interferometer. The main interferometer adopts the Mach-Zehnder interferometer structure, while the auxiliary interferometer adopts the Michelson interferometer structure. The source is a TLS, whose frequency increases linearly over time. The light from the TLS propagates through a coupler, splitting part of the

power into the main interferometer to obtain a longer sensing distance. While the other power enters the auxiliary interferometer, which is reflected by two Faraday rotation mirrors (FRMs), passes through different distance optical fibers and forms a reference beat signal in the coupler 4. Then the beat signal is received by the photodetector (PD). In the main interferometer, the backward Rayleigh signal and local light generated by the fiber under test form the actual test signal in coupler 3. The polarization beam splitter (PBS) then splits the signal into two mutually perpendicular polarized states, which are received by the balanced photodetector (BPD). Finally, the data collected by the data acquisition card (DAQ) is transferred to the computer.

In the simulation, the linear sweep rate is fixed as 6.25 GHz/s, and the corresponding wavelength scanning rate is 5 nm/s (the central wavelength is 1 550 nm). The signal to noise ratio (SNR) of the strong reflection point is 20 dB. In order to introduce the nonlinear phase noise of laser source, a wave interference term is added $r_n = A_n \cos(2\pi f_n t)$, whose intensity is determined by A_n and f_n .

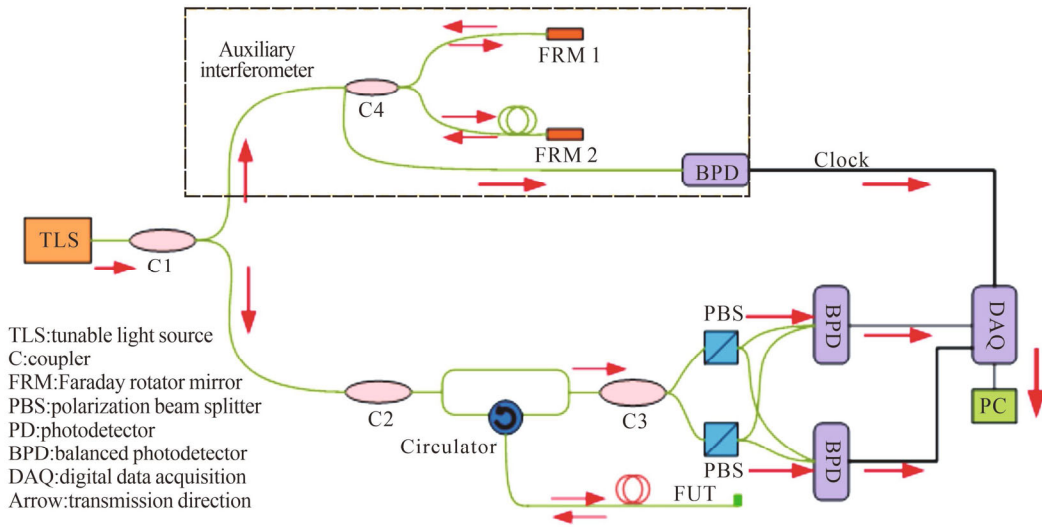


Fig.2 Simulation structure of optical frequency domain reflectometry system

Theoretically, for the distributed sensing system based on OFDR, the spatial resolution Δz in space domain is determined and calculated by the effective scanning spectral range Δf_{scan} of the TLS^[15] as

$$\Delta z \cong \frac{c}{2n_g \Delta f_{\text{scan}}}, \quad (14)$$

where c refers to the light velocity in a vacuum, and n_g is the group refractive index of the fiber.

The simulation results are shown below. After the nonlinear compensation based on the PRA, it can be seen from Fig.3 that the algorithm can effectively eliminate the nonlinear phase noise and obtain a clear reflection point, and it is obvious that the spatial resolution is about 50 cm in this algorithm. The effective spatial resolution is approaching the theoretical spatial resolution.

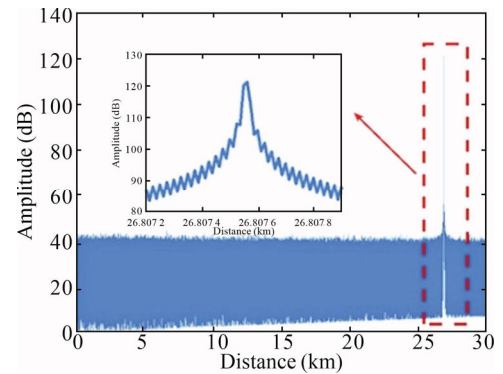


Fig.3 Measured Rayleigh backscattering after compensation by the PRA (Inset: the enlarge image of the reflection point)

For the confirmation of strain position, the cross-correlation algorithm is adopted in this paper to judge the position of disturbance by evaluating the similarity between the reference signal and the measurement signal. When disturbance-free and disturbance-free signals are cross-correlated, their similarity degree will be very high, which will produce a significant cross-correlation peak in the data center. However, the phase modulation of the signal can be generated due to vibration, which produces many additional frequency components, resulting in very low similarity. Therefore, there will be many miscellaneous peaks around the cross-correlation peak when there are a disturbance and a disturbance-free signal for cross-correlation operation. As shown in Fig.4(a), the two signals are cross-correlated in the time domain without disturbance. At this point, we can find that the cross-correlation results are triangular and have a significant peak in the middle. In the case of disturbance, the amplitude of cross-correlation results is small and the peak value is not obvious. In the frequency domain, as shown in Fig.4(b), the cross-correlation results show a single peak in the absence of disturbance, while in the presence of disturbance, there are multiple miscellaneous peaks.

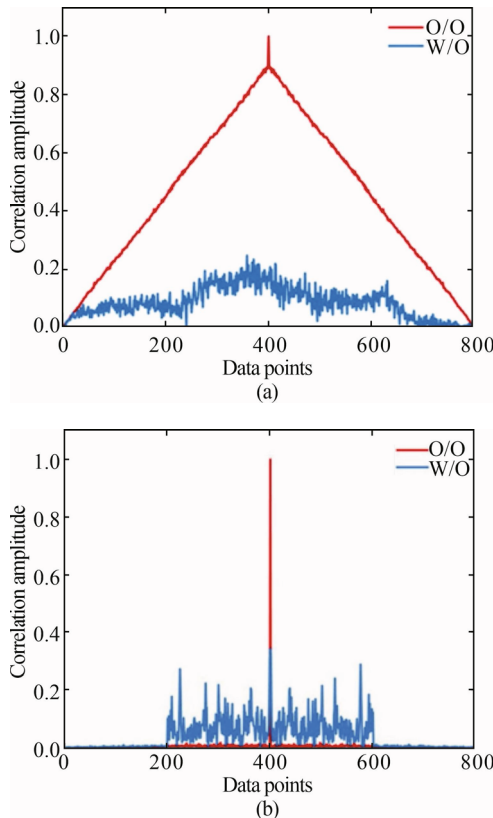


Fig.4 Cross-correlation results of (a) time domain and (b) frequency domain with and without disturbance

Fig.5 presents demodulation results with different modulation depths. To verify the effect of modulation depth on the demodulation results, we use different modulation depths as comparisons. Fig.5 shows whether C is set to 2.37 or 2.63, the change of modulation depth has no significant effect on the demodulation results. Meanwhile, the improved algorithm realizes perfect demodulation without harmonic distortion, which is consistent with the previous theoretical analysis.

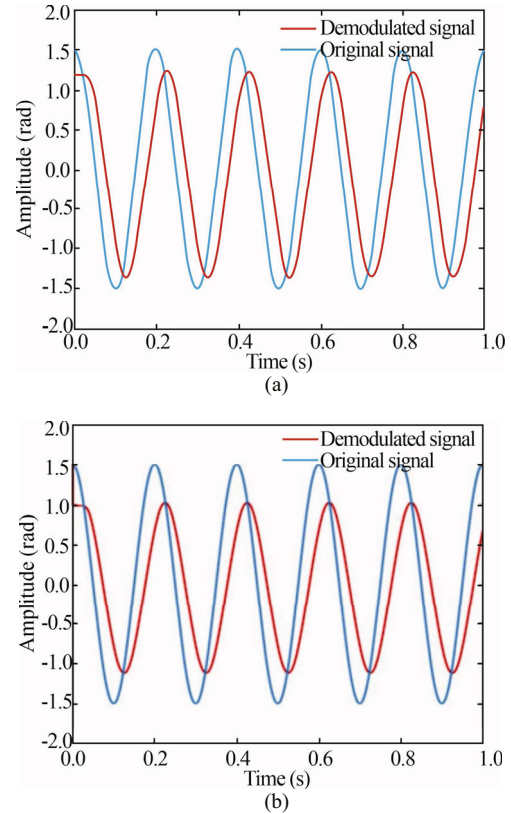


Fig.5 Demodulation results with different modulation depths: (a) $C=2.37$; (b) $C=2.63$

By analyzing the phase variation of Rayleigh back-scattered light, the strain information is directly demodulated in this paper. For static strain demodulation, as shown in Fig.6, we can observe that the strain increases from $1.3\mu\epsilon$ to $4.0\mu\epsilon$ in the range from 269.8 m to 270 m, and the minimum strain resolution reaches $0.3\mu\epsilon$. In the undisturbed region, the amplitude of demodulation results is small and almost negligible. In the disturbed region, we can obtain the peak value corresponding to the magnitude of the strain. According to the demodulation result, the amplitude of noise variation fluctuates within a certain range and the maximum detection error is about $0.5\mu\epsilon$. Therefore, it can be confirmed that the distributed sensing system based on OFDR proposed in this paper can realize high precision static strain sensing.

The results of dynamic strain demodulation with different amplitudes are shown in Fig.7. It can be found that the distributed sensor proposed in this paper can have a better demodulation effect on dynamic strain of different

amplitude. As shown in Fig.7, when the strain signal is a cosine signal with an amplitude of $1\mu\epsilon$, the frequency of the demodulation signal is consistent with the strain signal, the amplitude is slightly different, and there is no harmonic distortion, which realizes the correct demodulation. When we change the signal amplitude, the demodulation performance is still good, but the amplitude has slightly deviated. Therefore, we can prove that the distributed sensing system based on phase-sensitive OFDR can achieve good dynamic strain sensing performance.

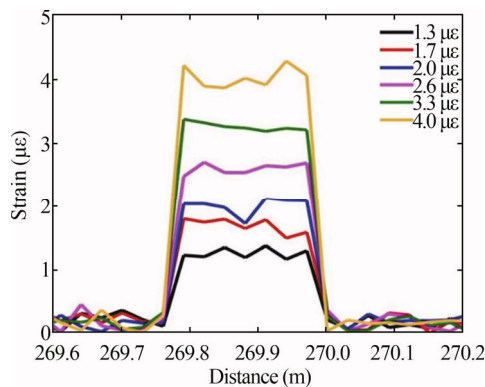


Fig.6 Static strain detection results by phase demodulation scheme based on ARC-DSM algorithm

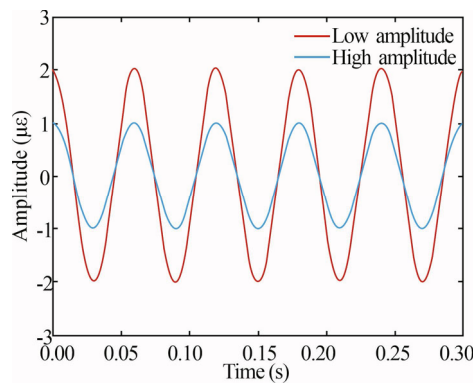


Fig.7 Dynamic strain demodulation results with different amplitudes

A high precision distributed strain optical fiber sensor based on phase-sensitive OFDR is proposed in this paper. Unlike the traditional method of indirectly realizing strain sensing through cross-correlation peak offset, this method directly demodulates strain information by analyzing phase changes of Rayleigh backscattered light. Simulation results show that the system can make the static strain resolution reach about $0.3\mu\epsilon$ and the spatial resolution can reach 0.2 m within 270 m range.

Statements and Declarations

The authors declare that there are no conflicts of interest related to this article.

References

- [1] LUO M M, LIU J F, TANG C J, et al. 0.5mm spatial resolution distributed fiber temperature and strain sensor with position-deviation compensation based on OFDR[J]. *Optics express*, 2019, 27(24): 35823-35829.
- [2] EICKHOF W, ULRICH R. Optical frequency domain reflectometry in single mode fiber[J]. *Applied physics letters*, 1981, 9 (39): 693-695.
- [3] FAN X, KOSHIKIYA Y, ITO F. Phase-noise-compensated optical frequency-domain reflectometry[J]. *IEEE journal of quantum electronics*, 2009, 45(6): 594-602.
- [4] FROGGATT M, MOORE J. High-spatial-resolution distributed strain measurement in optical fiber with Rayleigh scatter[J]. *Applied optics*, 1998, 37(10): 1735-1740.
- [5] CHEN D, LIU Q, HE Z. Phase-detection distributed fiber-optic vibration sensor without fading-noise based on time-gated digital OFDR[J]. *Optics express*, 2017, 25(7): 8315.
- [6] LI J, GAN J, ZHANG Z, et al. High spatial resolution distributed fiber strain sensor based on phase-OFDR[J]. *Optics express*, 2017, 25(22): 27913.
- [7] LO Y L, CHUANG C H. New synthetic-heterodyne demodulator for an optical fiber interferometer[J]. *IEEE journal of quantum electronics*, 2001, 37(5): 658-663.
- [8] ZHANG A L, WANG K H, ZHANG S, et al. All-digital demodulation system of interferometric fiber optic sensors using an improved PGC algorithm based on fundamental frequency mixing[J]. *Optoelectronics letters*, 2015, 11(3): 222-225.
- [9] BUCARO J A. Fiber-optic hydrophone[J]. *Journal of the acoustical society of America*, 1977, 62(5): 1302-1304.
- [10] WANG G Q, XU T W, FANG L. PGC demodulation technique with high stability and low harmonic distortion[J]. *IEEE photonics technology letters*, 2012, 24(23): 2093-2096.
- [11] HUANG S C, HUANG Y F, WU Z Z. Sensitivity normalization technique of PGC demodulation with low harmonic distortion and high stability using laser modulation to generate carrier signal[J]. *Sensors and actuators A physical*, 2012, 174: 198-206.
- [12] YANG L, WANG L, TIAN C, et al. Analysis and optimization of the PGC method in all digital demodulation systems[J]. *Journal of lightwave technology*, 2009, 26(18): 3225-3233.
- [13] WU Y, GAN J, LI Q, et al. Distributed fiber voice sensor based on phase-sensitive optical time-domain reflectometry[J]. *IEEE photonics journal*, 2015, 7(6): 1-10.
- [14] FAN X J, LIU J F, LUO M M, et al. A method for nonlinearity compensation of OFDR based on polynomial regression algorithm[J]. *Optoelectronics letters*, 2020, 16(2): 108-111.
- [15] SANG A K, FROGGATT M E, GIFFORD D K, et al. One centimeter spatial resolution temperature measurements in a nuclear reactor using Rayleigh scatter in optical fiber[J]. *IEEE sensors journal*, 2008, 8(7): 1375-1380.